

PPPL-CFP--3927

PHYSICAL PROCESSES OF SUBSTORM ONSET AND CURRENT
DISRUPTION OBSERVED BY AMPTE/CCE

COWF-9803142--

C. Z. Cheng

Princeton Plasma Physics Laboratory, Princeton University
Princeton, NJ 08543

A. T. Y. Lui

Applied Physics Laboratory, Johns Hopkins University
Laurel, MD 20723

Abstract. A new scenario of AMPTE/CCE observation of substorm onset and current disruption and the corresponding physical processes is presented. Toward the end of late growth phase plasma β increases to ≥ 50 and a low frequency instability with a wave period of 50 – 75 seconds is excited and grows exponentially to a large amplitude at the onset of current disruption. At the current disruption onset higher frequency instabilities are excited so that the plasma and electromagnetic field form a turbulent state. Plasma transport and heating take place to reduce plasma β and modify the ambient plasma pressure and velocity profiles so that the ambient magnetic field recovers from a tail-like geometry to a more dipole-like geometry. To understand the excitation of the low frequency global instability, a new theory of kinetic ballooning instability (KBI) is proposed to explain the high critical β threshold ($\beta_c \geq 50$) of the low frequency global instability observed by the AMPTE/CCE. The stabilization kinetic effects of trapped electron and finite ion Larmor radii give rise to a large parallel electric field and hence a parallel current that greatly enhances the stabilizing effect of field line tension to the ballooning mode. As a result β_c for excitation of KBI is greatly increased over the ideal MHD ballooning instability threshold by $\geq O(10^2)$. The wave-ion magnetic drift resonance effect typically reduces β_c by up to 20% and produces a perturbed resonant ion velocity distribution with a duskward velocity roughly equal to the average ion magnetic (∇B and curvature) drift velocity as the KBI grows to a large amplitude ($\delta B/B \geq 0.3$). Higher frequency instabilities such as cross-field current instability (CCI) can be excited by the additional velocity space free energy associated with the positive slope in the perturbed resonant ion velocity distribution.

1. Introduction

A critical process in the previously established view of the substorm onset and current disruption based on the observation of AMPTE/CCE spacecraft is the explosive growth phase (which lasts ~ 30 seconds) at the approach of current disruption onset [Ohtani *et al.*,

1992]. During the explosive growth phase a large surge in the duskward ion bulk drift to nearly the ion thermal velocity is found near the local midnight sector which could lead to the excitation of the cross-field current instability (CCI) during the cross tail current disruption phase [Lui, 1996]. In this paper a new scenario of the AMPTE/CCE observation of substorm explosive growth phase, onset and current disruption is presented. In particular, toward the end of late growth phase (approximately 2 minutes before the onset of current disruption) plasma pressure becomes isotropic and β increases to ≥ 50 and we have found that a low frequency global instability with a wave period of ~ 50 –75 seconds is excited and grows exponentially to a large amplitude with $\delta B/B \geq 0.3$ at the onset of current disruption. The half wave period of the instability before the current disruption onset corresponds to the explosive growth phase. At the current disruption onset higher frequency instabilities (with wave periods 15 sec, 10, sec, 5 sec, etc.) are excited and the plasma and electromagnetic field form a strong turbulent state for ~ 4 –5 minutes. During the strong turbulent state anomalously fast plasma transport and heating take place to modify the average plasma pressure and flow profiles so that the ambient magnetic field recovers from a tail-like geometry to a more dipole-like geometry.

Two key issues need to be resolved in order to further understand the physical processes of the current disruption and subsequent magnetic field dipolarization: (1) the excitation mechanism and the high plasma β threshold (≥ 50) of the low frequency global instability that underlines the explosive growth phase; (2) the physical mechanism of the enhanced ion drift in the explosive growth phase that leads to excitation of higher frequency instabilities. To understand these two key issues, we have developed a new theory of kinetic ballooning instability (KBI), which results from the release of configuration space ballooning free energy of nonuniform pressure with gradient in the same direction as the magnetic field curvature. Previously ballooning instability based on ideal MHD model has been proposed to explain the current disruption [Roux *et al.*, 1991]. Ideal MHD ballooning mode theory would predict a low β_c

DISCLAIMER

This report was prepared as an account of work sponsored by an agency of the United States Government. Neither the United States Government nor any agency thereof, nor any of their employees, makes any warranty, express or implied, or assumes any legal liability or responsibility for the accuracy, completeness, or usefulness of any information, apparatus, product, or process disclosed, or represents that its use would not infringe privately owned rights. Reference herein to any specific commercial product, process, or service by trade name, trademark, manufacturer, or otherwise does not necessarily constitute or imply its endorsement, recommendation, or favoring by the United States Government or any agency thereof. The views and opinions of authors expressed herein do not necessarily state or reflect those of the United States Government or any agency thereof.

DISCLAIMER

Portions of this document may be illegible in electronic image products. Images are produced from the best available original document.

(≤ 1) for instability, which is contrary to the high β values (≥ 20) observed by AMPTE/CCE throughout the late growth phase. In this paper we show that kinetic effects such as trapped particle dynamics, finite ion Larmor radii (FLR) and wave-particle resonances are important in determining the stability of KBI and we are able to answer these two key issues of substorm onset and current disruption.

The kinetic ballooning instability theory properly explains the wave frequency, growth rate and high β_c (≥ 50) of the low frequency instability observed by the AMPTE/CCE. Because the wave phase velocity along the field line is smaller than the electron thermal velocity, the trapped electron effect coupled with ion FLR effects causes a large parallel electric field and thus a much enhanced parallel current which greatly enhances the stabilizing field line tension over the value expected from the MHD theory. As a result, a much higher β_c than that based on the ideal MHD model is obtained with $\beta_c \geq O(10^2)\beta_c^{MHD}$, where β_c^{MHD} is the critical β predicted by the MHD theory. The effect of the wave-ion magnetic drift resonance with $\omega - \omega_{di} = 0$, where ω_{di} is the ion magnetic drift frequency, provides an additional channel to release the free energy and typically reduces β_c by up to 20%.

Another consequence of the wave-particle resonance is to produce a localized perturbed ion distribution in the velocity space centered around $v_y = v_{di}$, where v_y is the particle velocity in the dusk direction and v_{di} is the average ion magnetic (∇B and curvature) drift velocity. As KBI grows to a large amplitude, the perturbed ion velocity distribution increases so that $\partial f_i / \partial v_y > 0$ for $v_y \leq v_{di}$, which provides an additional free energy source for higher frequency instabilities such as CCI. As the higher frequency instabilities quickly grow to large amplitudes, they combine with KBI to form a strongly plasma turbulence, which leads to anomalously large plasma transport and heating in the current disruption phase. In a few minutes the plasma β decreases and the pressure profile relaxes to a more quiet time-like profile and the magnetic field recovers to a more dipole-like geometry. Thus, the new substorm scenario emphasizes a global low-frequency mode (KBI) which can naturally account for the explosive growth phase and the initiation of subsequent current disruption through a combination of KBI and CCI.

2. Low Frequency Global Instability Observed by AMPTE/CCE

Evidence for the low-frequency perturbations occurring prior to current disruption onset can be found in detailed examination of magnetic field during current disruption events. Figure 1 shows the result of such an analysis. Magnetic field measurements from AMPTE/CCE on August 30, 1986 were studied. The satellite was in the midnight local time sector, MLT = 23.5, at a radial distance of approximately $8R_E$. The current disruption onset time is determined to be at

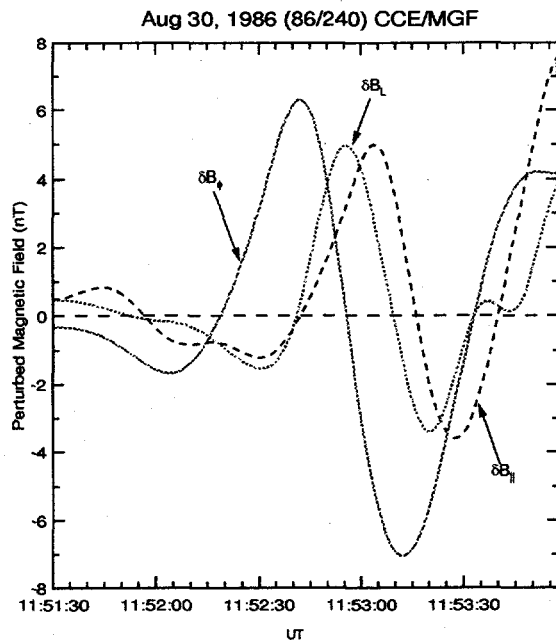


Figure 1. Three components of the low frequency perturbed magnetic field.

11:52:40 UT [Takahashi *et al.*, 1987; Lui *et al.*, 1992; Ohtani *et al.*, 1995]. To extract the low frequency components of the fluctuations, we employed successive smoothing of the original signals with normalized binomial coefficients as previously used in [Lui and Najmi, 1997]. The derived magnetic field perturbations in the cylindrical (V , D , H) components were then converted into components in the unperturbed magnetic field coordinate system to give δB_L , δB_ϕ , and δB_\parallel , where positive δB_ϕ is pointing eastward, positive δB_\parallel is along the mean magnetic field direction and positive δB_L is in the third right-handed orthogonal direction. From Figure 1, one can deduce that the real frequency of the low-frequency perturbation is ~ 0.1 Hz (compared with proton cyclotron frequency of about 1 Hz) and the growth rate is about 0.2 of the real frequency. Note that the exponentially low-frequency perturbation begins quite early at $\sim 11:51:30$ UT, ~ 1.5 min before the onset of current disruption. It is interesting to note that there is almost no magnetic field fluctuation before the low frequency global instability was observed. Although not shown here, the general characteristics of the low frequency perturbation given here are also found in another current disruption event (June 1, 1985) [Lui *et al.*, 1992] which we have examined.

The 30sec exponential growth phase period of the low frequency global instability (with amplitude reaching $\delta B/B \geq 0.3$) just before the current disruption onset was previously called "explosive growth phase" [Ohtani *et al.*, 1992] which is accompanied by a large duskward shift of the ion velocity distribution function and hence a significantly enhanced cross-tail current density [Lui, 1996]. This enhanced cross-tail ion drift

population is responsible for exciting higher frequency instabilities such as CCI which together with the low frequency global instability last through out the current disruption phase and form a strong turbulent state.

During the late growth phase of substorms the plasma pressure in the midnight sector of the near-Earth tail ($\sim 7-9R_E$) observed by the AMPTE/CCE [Lui *et al.*, 1992] usually increases $\sim 50\%$ from ~ 10 minutes prior to the current disruption onset to the time the low frequency global instability is observed. The corresponding plasma β usually increases from ~ 10 to ≥ 60 . This pressure change leads to cross-tail current enhancement and thinning of the plasma sheet. Although there is no observational determination on the pressure profile during the late growth phase, it is reasonable to expect that the plasma pressure decreases monotonically with increasing radial distance. Energy associated with the current enhancement can be viewed as being stored in the large-scale magnetic field on the nightside.

3. Kinetic Ballooning Instability

Based on the AMPTE/CCE observation of particle data [Lui *et al.*, 1992; Lui, 1996], at the end of the growth phase the average electron energy is about $5keV$ and the average ion energy is about $10keV$. The particle velocity distribution function does not have appreciable bulk drift and the plasma pressure becomes isotropic in the late growth phase in a few minutes before the onset. The average ion magnetic drift velocity evaluated at the average ion energy is about the same as the ion thermal velocity if the ∇B scale length is on the order of average ion Larmor radius. With these information we consider KBI perturbations with the orderings: $k_\perp \rho_i \sim O(1)$ and $k_\parallel \ll k_\perp$ and $v_{the} > (\omega/k_\parallel) > v_{thi}$ [Cheng, 1982b, 1982a], where the subscripts \parallel and \perp represent parallel and perpendicular components to the equilibrium magnetic field, respectively. With these orderings the following kinetic effects must be considered: trapped electron dynamics, ion FLR effect and wave-particle resonance with $\omega - \omega_{di} = 0$. We shall obtain approximate solutions of the perturbed particle distributions based on the gyrokinetic formulation by assuming that both electrons and ions have local Maxwellian equilibrium distribution functions [Cheng *et al.*, 1995].

We shall consider a three-dimensional magnetospheric equilibrium with the magnetic field expressed as $\mathbf{B} = \nabla\psi \times \nabla\alpha$, where ψ is chosen as the magnetic flux function which is a function of L -shell only and α is an azimuthal-angle like variable with a period of 2π . The guiding center particle equilibrium distribution is assumed to be $F = F(\mathcal{E}, \psi)$ so that the equilibrium pressure is a function of ψ only. We consider perturbations with $k_\parallel L_\parallel > 1$ and $k_\perp L_\perp > 1$, and $L_\parallel > L_\perp$, where $L_{\parallel,\perp}$ are the parallel and perpendicular background equilibrium scale lengths respectively. We assume a WKB eikonal representation for perturbed quantities, i.e., $\delta f(\vec{x}, \vec{v}, t) = \delta f(\mathbf{s}, \mathbf{k}_\perp, \vec{v}, t) \exp[i(\int d\vec{x}_\perp \cdot \mathbf{k}_\perp - \omega t)]$.

Including full FLR effects the perturbed particle distribution function can be expressed in terms of the rationalized MKS unit as $\delta f = (q/M)\partial F/\partial \mathcal{E}[(\omega_\star^T/\omega)\Phi - (1 - \omega_\star^T/\omega)(1 - J_0 e^{i\delta L})\Phi + g e^{i\delta L}]$, where M is the particle mass, q is the particle charge, B is the magnetic field intensity, $\delta L = \mathbf{k} \times \mathbf{v} \cdot \hat{\mathbf{b}}/\omega_c$, J_l is the l -th order Bessel function of the argument $k_\perp v_\perp/\omega_c$, $\omega_c = qB/M$ is the cyclotron frequency, Φ is the perturbed electrostatic potential, and g is the nonadiabatic part of the perturbed distribution function. Based on the WKB-ballooning formalism the lowest order gyrokinetic equation for g in the low frequency ($\omega \ll \omega_c$) limit is given by

$$(\omega - \omega_d + i\mathbf{v}_\parallel \cdot \nabla_\parallel)g = -\frac{q}{M} \frac{\partial F}{\partial \mathcal{E}} \left(1 - \frac{\omega_\star^T}{\omega}\right) \times \left[(\omega_d \Phi - i\mathbf{v}_\parallel \cdot \nabla_\parallel \Psi) J_0 + \frac{\omega v_\perp}{k_\perp} J_1 \delta B_\parallel \right], \quad (1)$$

where Ψ is the parallel perturbed electric field potential with $\mathbf{E}_\parallel = -\nabla_\parallel \Psi$, δB_\parallel is the parallel perturbed magnetic field, $\omega_\star^T = \mathbf{B} \times \mathbf{k}_\perp \cdot \nabla F / (B\omega_c \partial F / \partial \mathcal{E})$, $\omega_d = \mathbf{k}_\perp \cdot \mathbf{v}_d$ is the magnetic drift frequency, $\mathbf{v}_d = (\mathbf{B}/B\omega_c) \times (v_\parallel^2 \boldsymbol{\kappa} + \mu \nabla B)$ is the magnetic drift velocity, and $\boldsymbol{\kappa}$ is the magnetic field curvature. Note that the vector potential, defined by $\mathbf{A} = \mathbf{A}_\parallel - i\mathbf{A}_\perp \mathbf{B} \times \mathbf{k}_\perp / (Bk_\perp)$, is related to Φ , Ψ and δB_\parallel by $\omega \mathbf{A}_\parallel = -i\nabla_\parallel (\Phi - \Psi)$ and $\delta B_\parallel = k_\perp A_\perp$. We note that the gyrokinetic formulation is still valid for the case $\rho_i \sim L_\perp$ if the magnetic drift frequency is replaced with the pitch angle average value to account for the non-conservation of the magnetic moment [Hurricane *et al.*, 1994].

For electrons we shall neglect FLR effects and consider $|v_\parallel \nabla_\parallel| \gg \omega, \omega_{de}$. Clearly, trapped and un-trapped electrons have very different parallel dynamics. The un-trapped electron dynamics is mainly determined by its fast parallel transit motion, and to the lowest order in $(\omega/|v_\parallel \nabla_\parallel|)$ we obtain g_{eu} [Cheng, 1982a]

$$g_{eu} \simeq \frac{eF_e}{T_e} \left(1 - \frac{\omega_{*e}}{\omega}\right) \Psi, \quad (2)$$

where $\omega_{*e} = \mathbf{B} \times \nabla N_e \cdot \mathbf{k}_\perp / (B\omega_{ce} N_e)$ is the electron diamagnetic drift frequency, and the perturbed un-trapped electron density is given by

$$\delta n_{eu} = \frac{eN_{eu}}{T_e} \left[\frac{\omega_{*e}}{\omega} \Phi + \left(1 - \frac{\omega_{*e}}{\omega}\right) \Psi \right], \quad (3)$$

where $N_{eu}/N_e = 1 - [1 - B(s)/B_i]^{1/2}$ is the fraction of un-trapped electron at the field line location s , B_i is the magnetic field at the ionosphere. Near the equator $N_{eu}/N_e \simeq B(s)/2B_i \ll 1$. To carry out the velocity space integration, we have employed as the velocity space coordinates, v , λ , and σ , where $\lambda = h(s)v_\perp^2/v^2$, $h(s) = B_0/B(s)$, and B_0 is a reference magnetic field intensity defined by $B_0^{-1} = \int_{s_1}^{s_2} ds/B(s)$ and s_1 and s_2 are the fieldline locations at the southern and northern hemispheric ionospheres, respectively. In terms of these variables we have

$$\int d^3v = \sum_\sigma \pi \int_0^\infty dv v^2 \int_0^h \frac{d\lambda}{[h(h-\lambda)]^{1/2}}. \quad (4)$$

Un-trapped particles correspond to $0 \leq \lambda \leq h_m$ and trapped particles to $h_m \leq \lambda \leq h$ at a given field line location s , where h_m is the minimum value of $h(s)$ along a field line.

The trapped electron dynamics is mainly determined by its fast parallel bounce motion and to the lowest order in (ω/ω_{be}) [Cheng, 1982a; Cheng et al., 1995]

$$g_{et} \simeq \frac{eF_e}{T_e} \frac{\omega - \omega_{*e}^T}{\omega} \left[\Psi - \frac{\langle (\omega - \omega_{de}) \Psi \rangle}{\omega - \langle \omega_{de} \rangle} + \frac{\omega}{\omega - \langle \omega_{de} \rangle} \left\langle \frac{\omega_{de}}{\omega} \Phi + \frac{v_{\perp}^2 \delta B_{\parallel}}{2\omega_{ce}} \right\rangle \right], \quad (5)$$

where $\langle \omega_{de} \rangle$ represents the trapped particle orbit average of ω_{de} . The perturbed trapped electron density is given by

$$\delta n_{et} \simeq \frac{eN_{et}}{T_e} \left[\frac{\omega_{*e}}{\omega} \Phi + \left(1 - \frac{\omega_{*e}}{\omega}\right) \Delta \Psi \right] + \delta \hat{n}_{et}, \quad (6)$$

where $N_{et}/N_e = [1 - B(s)/B_i]^{1/2}$ is the fraction of trapped electron,

$$\Delta = \int_{tr} d^3v \frac{F_e}{N_{et}} \left[1 - \frac{\langle (\omega - \omega_{de}) \Psi \rangle}{\langle \omega - \omega_{de} \rangle \Psi} \right], \quad (7)$$

$$\delta \hat{n}_{et} = - \int_{tr} d^3v \frac{eF_e}{T_e} \frac{\omega - \omega_{*e}^T}{\omega - \langle \omega_{de} \rangle} \left\langle \frac{\omega_{de}}{\omega} \Phi + \frac{v_{\perp}^2 \delta B_{\parallel}}{2\omega_{ce}} \right\rangle. \quad (8)$$

Note that $\Delta \ll 1$ near the equator.

To obtain perturbed ion distribution function we assume that $\omega, \omega_{di} \gg |v_{\parallel} \nabla_{\parallel}|$, and the nonadiabatic perturbed distribution function is given by

$$g_i \simeq \frac{eF_i}{T_i} \frac{\omega - \omega_{*i}^T}{\omega - \omega_{di}} \left(\frac{\omega_{di} J_0 \Phi}{\omega} + \frac{v_{\perp} J_1 \delta B_{\parallel}}{k_{\perp}} \right). \quad (9)$$

Note that the ion dynamics is mainly determined by its perpendicular motion and the perturbed ion density is given by

$$\delta n_i = - \frac{eN_i}{T_i} \left[\frac{\omega_{*i}}{\omega} + \left(1 - \frac{\omega_{*i}}{\omega}\right) (1 - \Gamma) \right] \Phi + \delta \hat{n}_i, \quad (10)$$

where $\omega_{*i} = \mathbf{B} \times \nabla N_i \cdot \mathbf{k}_{\perp} / (B\omega_{ci}N_i)$, $\omega_{*pi} = \mathbf{B} \times \nabla P_i \cdot \mathbf{k}_{\perp} / (B\omega_{ci}P_i)$, $b_i = k_{\perp}^2 T_i / M_i \omega_{ci}^2 = k_{\perp}^2 \rho_i^2 / 2$, I_0 is the modified Bessel function of the zeroth order, and $\delta \hat{n}_i = \int d^3v g_i J_0$.

From the charge quasi-neutrality condition we obtain the parallel electric field potential

$$\left(\frac{N_{eu} + N_{et} \Delta}{N_e} \right) \Psi = - \frac{T_e}{T_i} \frac{\omega - \omega_{*pi}}{\omega - \omega_{*e}} (1 - \Gamma) \Phi + \frac{T_e}{eN_e} (\delta \hat{n}_i - \delta \hat{n}_e) \quad (11)$$

In comparison with the limit without trapped electron effects, the parallel electric field is enhanced by $N_e / (N_{eu} + N_{et} \Delta)$ which is much larger than unity near

the equator for $b_i \sim O(1)$. Making use of the parallel Ampere's law the perturbed parallel current is given by

$$\delta J_{\parallel} \simeq \frac{i}{\omega} \nabla_{\perp}^2 \nabla_{\parallel} (\Phi - \Psi) \simeq - \frac{k_{\parallel}}{\omega} \nabla_{\perp}^2 \times \left[1 + \frac{N_e T_e}{(N_{eu} + N_{et} \Delta) T_i} \frac{\omega - \omega_{*pi}}{\omega - \omega_{*e}} (1 - \Gamma) \right] \Phi, \quad (12)$$

which represents the enhancement of stabilizing field line tension due to effects of trapped electrons and ion FLR.

To obtain the eigenmode equation for ballooning instability we follow the derivation presented in the paper by Cheng et al. [1995]. By multiplying the gyrokinetic equation with particle charge, integrating it over the velocity space and summing it over all species, and making use of the parallel component of the Ampere's law we obtain

$$\mathbf{B} \cdot \nabla \left[\frac{k_{\perp}^2}{B^2} \mathbf{B} \cdot \nabla (\Phi - \Psi) \right] + \frac{\omega(\omega - \omega_{*pi})}{V_A^2} \frac{1 - \Gamma(b_i)}{\rho_i^2 / 2} \Phi + \frac{\mathbf{B} \times \boldsymbol{\kappa} \cdot \mathbf{k}_{\perp}}{B^2} \left(\frac{2\mathbf{B} \times \nabla P \cdot \mathbf{k}_{\perp}}{B^2} \Phi - \omega \sum_j \delta \hat{p}_j \right) = 0 \quad (13)$$

where $V_A = B / (n_i M_i)^{1/2}$ is the Alfvén speed, and the nonadiabatic perturbed pressures for each particle species are given by

$$\delta \hat{p}_j = M_j \int d^3v \left[\left(1 - \frac{\omega_{*j}^T}{\omega}\right) (1 - J_0^2) \Phi + g_j J_0 \right] \times \left(\frac{v_{\perp}^2}{2} + v_{\parallel}^2 \right). \quad (14)$$

Note that the relation $\mathbf{B} \cdot \delta \mathbf{B} + \delta P_{\perp} \simeq 0$ is used for low frequency instabilities with $\omega \ll k_{\perp} V_A$ [Cheng, 1991; Cheng and Qian, 1994; Cheng et al., 1995].

Equations (11) and (13) form a coupled set of kinetic ballooning eigenmode equations for solving Φ and Ψ along the field lines and the eigenvalue ω . We also need to obtain the nonadiabatic contributions of perturbed electron density, $\delta \hat{n}_{et}$ and $\delta \hat{n}_i$, and perturbed particle pressure $\delta \hat{p}_j$. The eigenmode equations include kinetic effects of trapped electron dynamics, parallel electric field, full ion FLR, and wave-particle resonances. Considering the ordering $\omega \gg \omega_{de}, \omega_{di}$, the nonadiabatic density and pressure responses in Eqs. (11) and (13) can be neglected and we obtain a kinetic ballooning mode equation that retains the trapped electron and ion FLR effects, and the local dispersion relation for KBI is approximately given by

$$\frac{\omega(\omega - \omega_{*pi})}{(1 + b_i) V_A^2} \simeq S k_{\parallel}^2 - \frac{2\boldsymbol{\kappa} \cdot \nabla P}{B^2}, \quad (15)$$

where $S = 1 + (b_i / (1 + b_i)) N_e T_e / (N_{eu} + N_{et} \Delta) T_i \gg 1$, and we have adopted the Padé approximation $1 - \Gamma \simeq b_i / (1 + b_i)$. The real frequency of KBI is $\omega_r = \omega_{*pi} / 2$ and the critical β is given by

$$\beta_c \simeq S \beta_c^{MHD} + \frac{\omega_{*pi}^2 R_c L_p}{4(1 + b_i) V_A^2}, \quad (16)$$

where R_c is the radius of the magnetic field curvature and L_p is the pressure gradient scale length, and $\beta_c^{MHD} = k_{\parallel}^2 R_c L_p$ is the ballooning instability threshold based on the MHD theory. It has also previously been calculated that $\beta_c^{MHD} \simeq 0.2$ for a dipole field with $L_p = 1R_E$ at $L = 8$ [Cheng and Qian, 1994]. For a more tail-like field we expect that β_c^{MHD} will be even smaller. Note that based on the magnetic field and plasma parameters observed by AMPTE/CCE: $B = 10nT$, $T_e/T_i = 0.5$, $b_i = 0.5$, we have $S \simeq 10^2 - 10^3$, then $\beta_c \geq O(10^2)\beta_c^{MHD} \sim O(10)$, which is consistent with the AMPTE/CCE observation.

If $\omega \sim \omega_{di}$, the wave-ion magnetic drift resonance can modify the growth rate and critical β . To fully evaluate the effect of wave-ion magnetic drift resonance, we need to retain ion nonadiabatic responses in perturbed density and pressures. Numerical studies of KBI have been performed for tokamaks previously [Cheng, 1982b, 1982a] and the results indicated that the effect of the wave-ion magnetic drift resonance is to reduce β_c by at most 20% and the real frequency of KBI will increase to ω_{*pi} at critical β . We expect the results for the magnetosphere will be qualitatively similar to the tokamak case and the detailed numerical solutions will be presented in the future.

One consequence of the wave-ion magnetic drift resonance is that as KBI grows to a large value with $\delta B/B \geq 0.3$ the perturbed resonant ion velocity distribution has a positive slope near the duskward resonant ion magnetic drift velocity. This can be clearly seen from the $(\omega - \omega_{di})$ resonance denominator in the perturbed ion distribution. Because $\omega_r \simeq \omega_{*pi}/2$, the wave-ion magnetic drift resonance will occur at $v_{di} = T_i \mathbf{B} \times \nabla P_i / (2eP_i B^2) \simeq v_{thi} \rho_i / 2L_{pi}$, where ρ_i is the ion Larmor radius and L_{pi} is the ion pressure gradient scale length. Thus, $|v_{di}| \sim v_{thi}$ for $\rho_i \sim L_{pi}$.

4. Summary and Discussion

In this paper we have identified a new scenario and physical processes of substorm onset and current disruption observed by AMPTE/CCE. Approximately 2 minutes before the current disruption onset, a global kinetic ballooning instability with period of about 50–75 seconds is excited as the plasma β increases above a high threshold value of ≥ 50 . The plasma β in the growth phase is usually larger than 10 which is much larger than the ballooning mode β threshold based on the ideal MHD theory. As KBI grows to a large amplitude with $\delta B/B > 0.3$, the wave-ion resonance with $\omega - \omega_{di} = 0$ produces a perturbed ion distribution centered around $v_y \sim v_{di}$ and thus the full ion distribution function has a positive slope with $\partial F_i / \partial v > 0$ for $v_y \leq v_{di}$. The perturbed ion distribution provides the velocity space free energy to excite instabilities such as CCI. As these low and high frequency instabilities grow,

a strong plasma turbulence can be developed fully to yield large plasma transport (via diffusion, convection as well as magnetic reconnection) and heating. In a few minutes the plasma pressure profile averaged over the fast fluctuation time scales is changed so that the magnetic field recovers to a more dipole-like geometry that satisfies the force balance equation.

Acknowledgments This work is supported by the NSF Grants No. ATM-9523331 and No. ATM-9622080 and the DoE Contract No. DE-AC02-76-CHO3073.

References

- Catto, P. J., W. M. Tang, and D. E. Baldwin, Generalized gyrokinetics, *Plasma Phys.*, *23*, 639–650, 1981.
- Cheng, C. Z., High-n collisionless ballooning modes in axisymmetric toroidal plasmas, *Nucl. Fusion*, *22*, 773–781, 1982a.
- Cheng, C. Z., Kinetic theory of collisionless ballooning modes, *Phys. Fluids*, *25*, 1020–1026, 1982b.
- Cheng, C. Z., A kinetic-magnetohydrodynamic model for low-frequency phenomena, *J. Geophys. Res.*, *96*, 21,159–21,171, 1991.
- Cheng, C. Z., and Q. Qian, Theory of ballooning-mirror instabilities for anisotropic pressure plasmas in the magnetosphere, *J. Geophys. Res.*, *99*, 11,193–11,209, 1994.
- Cheng, C. Z., N. N. Gorelenkov, and C. T. Hsu, Fast particle destabilization of TAE modes, *Nucl. Fusion*, *35*, 1639–1650, 1995.
- Hurricane, O. A., R. Pellat, and F. V. Coroniti, The kinetic response of a stochastic plasma to low frequency perturbations, *Geophys. Res. Lett.*, *21*, 253, 1994.
- Lui, A. T. Y., Current disruption in the Earth's magnetosphere: Observations and models, *J. Geophys. Res.*, *101*, 13067, 1996.
- Lui, A. T. Y., and A.-H. Najmi, Time-frequency decomposition of signals in a current disruption event, *Geophys. Res. Lett.*, *24*, 3157, 1997.
- Lui, A. T. Y., et al., Current disruptions in the near-Earth neutral sheet region, *J. Geophys. Res.*, *97*, 1461, 1992.
- Ohtani, S., K. Takahashi, L. Zanetti, T. A. Potemra, R. W. McEntire, and T. Iijima, Initial signatures of magnetic field and energetic particle fluxes at tail reconfiguration: Explosive growth phase, *J. Geophys. Res.*, *97*, 19311, 1992.
- Ohtani, S., T. Higuchi, A. T. Y. Lui, and K. Takahashi, Magnetic fluctuations associated with tail current disruption: Fractal analysis, *J. Geophys. Res.*, *100*, 19135, 1995.
- Roux, A., S. Perraut, A. Morane, P. Robert, A. Korth, G. Kremser, A. Pederson, R. Pellinen, and Z. Y. Pu, Plasma sheet instability related to the westward traveling surge, *J. Geophys. Res.*, *96*, 17697, 1991.
- Takahashi, K., L. J. Zanetti, R. E. Lopez, R. W. McEntire, T. A. Potemra, and K. Yumoto, Disruption of the magnetotail current sheet observed by AMPTE/CCE, *Geophys. Res. Lett.*, *14*, 1019, 1987.

Correspondence to: C. Z. Cheng (Fax: 609-243-2662, E mail: fcheng@pppl.gov)